Nonreciprocal and Reciprocal Complex and Backward Waves in Parallel Plate Waveguides Loaded with a Ferrite Slab Arbitrarily Magnetized

Ricardo Marqués, Francisco L. Mesa, and Manuel Horno, *Member IEEE*

Abstract— **This paper presents a rigorous and systematic method of analysis of the electromagnetic wave propagation in parallel plate waveguides with a multilayered bianisotropic medium. The method is applied to the numerical study of parallel plate waveguides with a multilayered medium including lossless ferrite layers magnetized at an arbitrary direction. Both the propagation constant and the transmitted power are computed. Backward, i.e., power flux in opposite direction as phase velocity, and nonreciprocal complex modes have been found to be an essential part of the model spectrum of the structures analysed here. A detailed investigation has been carried out about the parameters related to the appearance of these modes.**

I. Introduction

In THE LAST four decades, the study of the interaction of microwaves with ferrites inside waveguides has steadily increased owing to its interest in the microwave technology. Propagation in planar ferrite-loaded structures for different dc magnetic bias orientation has been widely studied by means of a magnetostatic approach (eg., [1] and references therein). There are also some works in the literature dealing with the electromagnetic wave propagation in arbitrarily magnetized homogeneous ferrites between two perfectly conducting plates (see [2] and references therein) and some other works dealing with multilayered ferrite-loaded planar waveguides magnetized at a direction either parallel or orthogonal to the direction of propagation [3]–[5]. However, to the authors' knowledge, there is not any work devoted to the full-wave analysis of electromagnetic propagation in multilayered ferrite-loaded parallel plate waveguides arbitrarily magnetized. The relevance of an electromagnetic analysis, even if the normalized phase constant is high enough to apply the magnetostatic approach, has been shown in [6].

Another topic widely analyzed in the literature is the microwave propagation along microstrip or microslot-like transmission lines on ferrite-loaded substrates magnetized at different directions. Specifically, [7], [8] have analyzed electromagnetic propagation in microstrip-like structures printed on a general anisotropic substrate (including a ferrite slab with an arbitrary dc biasing magnetic field). These structures as well as most guide elements used in MIC/MMIC technology lines or image guides can be subdivided in regions that can be viewed as multilayered parallel plate waveguides. The knowledge of the different modes propagating at an arbitrary direction in these parallel plate waveguides is a very valuable point to be considered in the analysis of the MIC and MMIC lines. For example, the presence of leaky waves can be predicted from the knowledge of the modal spectrum of the different parallel plate subregions in which the line is subdivided [9], [10].

When magnetized ferrite layers are present in lines, the modal spectrum of the different parallel plate waveguides strongly depends on the direction of wave propagation in the plane of the structure (the plane defined by the planar nature of the structure). Notice that the direction fixed by the dc magnetizing field $\boldsymbol{H}_0$ determines a privileged direction in these waveguides on the contrary to what happens in nonmagnetized waveguides. Thus, the analysis of wave propagation at an arbitrary direction with respect to the direction fixed by $\boldsymbol{H}_0$ can be equally made by analyzing the wave propagation along a fixed direction but with the dc biasing field arbitrarily oriented. Therefore, the analysis of the modal spectrum of a ferrite loaded parallel plate waveguide, with an arbitrary dc magnetic biasing field, should be an essential previous step for the study of the propagation along fin-line and microstrip-like transmission lines printed in these waveguides, even in case the dc magnetization is either normal or parallel to the direction of propagation imposed by the metallizations.

In this paper, we present a systematic method to obtain the complete modal spectrum of a multilayered parallel plate waveguide arbitrarily magnetized, or in other words, the modes propagating at an arbitrary direction inside a parallel plate waveguide with a fixed dc magnetic bias field. The dispersion relation is obtained by following the basic ideas previously developed by the authors in [11] to compute the spectral Green's function of a planar structure with a multilayered bianisotropic medium. In this way, the dispersion relation is expressed in terms of solutions to certain equation that are shown to be the complex zeroes of an *analytical* function. This fact makes it possible to apply conventional and very efficient integral methods [12] to obtain *all* the roots of the

Manuscript received July 3, 1991; revised December 28, 1992. This work was supported by CICYT, Spain Under Grant TIC91-1018.

The authors are with the Grupo de Microondas, Departmento de Electronica Y Electromagnetismo, Universidad de Sevilla, Avda, Reina Mercedes, s/n, 41012-Sevilla, Spain.

IEEE Log Number 9201023̀3.

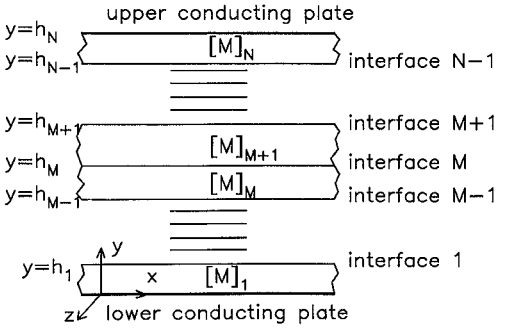

Fig. 1. Cross-section of a multilayered parallel plate waveguide.

dispersion equation in a given region of the complex plane. Transmitted power through each layer is also computed by using an analytical algorithm that is developed here.

The numerical analysis of the above structures has revealed the presence of certain unusual types of modes, namely nonreciprocal complex wave modes. Reciprocal complex modes have been reported in different shielded dielectric loaded waveguides such as circular waveguides containing an axial dielectric rod [14], rectangular image guides [15], fin-lines [16], and in microstrip lines [17], [18]. These modes also appear in waveguides homogeneously filled with anisotropic media [19]. The existence of nonreciprocal complex modes in transversely magnetized ferrite-loaded fin-lines was reported in [20].

More recently, the authors have shown that all modes that do not carry a net average power flux must be complex if they are also nonreciprocal and propagate along a transversely magnetized waveguide with an arbitrary cross-section [21]. In the present paper, the nonreciprocal complex modes are deeply analyzed in order to establish their main characteristics (frequency range and mechanism of appearance and disappearance, transmitted power, mode coupling, etc).

II. Analysis

A. Characteristic Equation

Consider the multilayered parallel plate waveguide shown in Fig. 1. The layers are assumed to be made of arbitrary bianisotropic materials, including in this way: dielectric or magnetic intrinsic anisotropy, optical activity, and magnetized ferrite and/or semiconductor—namely, gyrotropic layers. The unique restriction is that the media must show a linear electromagnetic behavior, i.e., the constitutive electromagnetic properties of each layer can be described by means of a 6×6 tensor:

$$\begin{bmatrix} \boldsymbol{D} \\ \boldsymbol{B} \end{bmatrix} = [\boldsymbol{M}]_i \cdot \begin{bmatrix} \boldsymbol{E} \\ \boldsymbol{H} \end{bmatrix}; \qquad [\boldsymbol{M}]_i = \begin{bmatrix} [\epsilon]_i & [\rho]_i \\ [\rho']_i & [\mu]_i \end{bmatrix}_{(6\times 6)} \tag{1}$$

with $[\epsilon]_i$ and $[\mu]_i$ being the dielectric permittivity and the magnetic permeability, respectively, and $[\rho]_i$, $[\rho']_i$ the optical activity tensors.

Let a new structure be formed by removing the upper conducting half plane of the structure in Fig. 1 and impressing a tangential electric field $\boldsymbol{E}_t^u = \boldsymbol{E}_{t,0}^u \exp(j\omega t - jk_z z - jk_x x)$ at this upper interface (k_z and k_x stand for the complex propagation constants in the $+z$ and $+x$ direction, respectively, and ω for the angular frequency; the time-dependence will not be written henceforth). It is followed from the uniqueness theorem that the electromagnetic field between upper and the lower interfaces of this new configuration is completely determined provided the tangential electric field at the upper boundary is imposed (the lower interface being a perfect conducting plate). Specifically, once the tangential magnetic field on the lower plane has been obtained, the surface currents on this conducting plate are determined. Owing to the linear properties of the media, a linear relation has to exist between the tangential electric field at the upper plane E_x^u, E_z^u, and the current on the lower conducting plane J_x^l, J_z^l, that is

$$\boldsymbol{J}_{t,0}^l = [\boldsymbol{L}(k_z, k_x, \omega)] \cdot \boldsymbol{E}_{t,0}^u . \tag{2}$$

Note that once (2) is stated, the characteristic equation can be readily obtained. This is made by requiring that a lower current surface do exist ($\boldsymbol{J}_{t,0}^l \neq 0$), if a null upper electric tangential field ($\boldsymbol{E}_{t,0}^u = 0$) is imposed. The characteristic equation can then be written by means of the following implicit relation:

$$\det\left([\boldsymbol{L}(k_z, k_x, \omega)]^{-1}\right) = 0 . \tag{3}$$

A direct comparison of (2) with expression (4) in [11] shows that the $[\boldsymbol{L}]$ matrix appearing in (2) is in fact the $[\boldsymbol{L}(k_z, k_x, \omega)]_{K,K+1}$ matrix defined in [11] in case the subscripts n_K and n_{K+1} (see [11, Fig. 3 (c)]) stand for the lower and upper planes of the current configuration, respectively. Hence, the $[\boldsymbol{L}]$ matrix of (2) can be computed following the general method developed in [11].

Fixed the value of ω, a pair of k_z, k_x satisfying (3) corresponds to a plane wave propagating in the parallel plate waveguide with a wave vector $\boldsymbol{k} = k_z \boldsymbol{a}_z + k_x \boldsymbol{a}_x$. Notice that the wave-vector $\boldsymbol{k} = k_x \boldsymbol{a}_x + k_z \boldsymbol{a}_z$ does not always define a direction in the $(x-z)$ plane since the quantities k_z, k_x are in general complex. Only in few cases (for example when both k_z and k_x are real) $\boldsymbol{k}$ does define a direction in the $(x-z)$ plane ($\boldsymbol{k} = k_\xi \boldsymbol{a}_\xi$; $\boldsymbol{a}_\xi$ is a unitary vector in the $(x-z)$ plane). Only in these cases the fields do not vary in the direction perpendicular to $\boldsymbol{a}_\xi$ and $\boldsymbol{a}_y$ (defined by $\boldsymbol{a}_\eta = \boldsymbol{a}_y \times \boldsymbol{a}_\xi$). This type of waves will be called in the following *uniform modes* since they are uniform in a direction that is perpendicular to the propagation one. Although in the numerical computations we restrict ourselves to the uniform modes defined above, the method developed here is not restricted by this limitation.

B. Solution of the Characteristic Equation

For fixed values of ω and k_x, the complex function $f(k_z) = \det\left([\boldsymbol{L}(k_z; k_x, \omega)]^{-1}\right)$ appearing in (3) is an *analytic* function in the complex k_z-plane. This relevant feature can be deduced from the fact that, any pole of the above function must be related to an electromagnetic field configuration in which both $\boldsymbol{a}_y \times \boldsymbol{E}$ and $\boldsymbol{a}_y \times \boldsymbol{H}$ vanish at the lower plane of Fig. 1, with a nonzero impressed tangential electric field at the upper plane (after the conducting plate at this plane has been removed). Nevertheless, it can be shown that this field configuration is not possible if the layers are made of linear media and have finite

thickness (see Appendix A). Therefore, the above function cannot have poles in the entire complex plane.

Being $f(k_z)$ an analytic function, it is possible to apply a contour integral method to search for the zeroes of (3) in the complex k_z plane. The method used in this work is base on the well known theorem of the theory of analytical functions which states that, if $f(k_z)$ is an analytical function, and C is a closed curve in the complex k_z plane that does not pass through a zero of $f(k_z)$, then

$$\frac{1}{2\pi}\oint_C k_z^N \frac{f'(k_z)}{f(k_z)}\,dk_z = \sum_{i=1}^{\nu} k_{z,i}^N \tag{4}$$

where $k_z, i(i=1,\cdots,\nu)$ are all the zeros of $f(k_z)$ that lie in the region enclosed by the curve C.

Starting from (4) it is possible to develop a *systematic* method for searching *all* the zeros of $f(k_z) = \det\big([\boldsymbol{L}(k_z;k_x,\omega)]^{-1}\big)$ in a given region of the complex k_z-plane. A general description of this method can be found in [12], nevertheless, we will give here a brief sketch of the specific procedure followed by us (more details about the implementation of the method are given in [13]). The contour integration is chosen to be a circumference and the numerical integration is made in terms of the Gauss–Legendre quadratures (a forty-points quadrature provides sufficient accuracy). We begin by computing (4) for $N=0$, obtaining in this way the total number of zeros ν within the region enclosed by C. If $\nu > 4$ the region is subdivided in subregions up to $\nu \le 4$. In this case, the integrals in (4) are computed for $N=1,\cdots,\nu$ to obtain a set of ν equations of order ν. The roots of these equations are the zeros of $f(k_z)$, $k_{z,i}, i=1,\cdots,\nu$ in the considered subregion. These roots can be algebraically obtained if $\nu \le 4$. The CPU time employed in the forty evaluations of $f(k_z) = \det\big([\boldsymbol{L}(k_z;k_x,\omega)]^{-1}\big)$ to compute the Gauss–Legendre quadrature, is about 200 milliseconds in a Vax-6410 machine.

If $k_{z,i}$ is a zero of $f(k_z) = \det\big([\boldsymbol{L}(k_z;k_x,\omega)]^{-1}\big)$ for a given k_x, the pair $(k_{z,i},k_x)$ defines a uniform mode propagating along the waveguide. Nevertheless, if we are only interested in obtaining the complex propagation constants k_ξ of the different uniform modes that can propagate along the structure at an arbitrary direction, $\boldsymbol{a}_\xi = \cos\xi\boldsymbol{a}_z + \sin\xi\boldsymbol{a}_x$, in the $(x-z)$ plane (namely, at an angle ξ with respect to the positive z direction), we only need to compute the zeros of $f(k_z) = \det\big([\boldsymbol{L}(k_z;0,\omega)]^{-1}\big)$ (with $k_x=0$), after the media and the dc biasing fields in Fig. 1 are subjected to a rotation by angle $-\xi$ about the z-axis.

C. Power Computation

The average powers per unit length transmitted in the x and z direction through each layer, i, of the structure shown in Fig. 1, $\mathcal{P}_z^{(i)}$ and $\mathcal{P}_x^{(i)}$, are given by

$$\mathcal{P}_z^{(i)} = \frac{1}{2}\,\Re\int_{h_{i-1}}^{h_i}\big(E_xH_y^* - E_yH_x^*\big)_i\,dy \tag{5}$$

$$\mathcal{P}_x^{(i)} = \frac{1}{2}\,\Re\int_{h_{i-1}}^{h_i}\big(E_yH_z^* - E_zH_y^*\big)_i\,dy \tag{6}$$

(superscript * indicates complex conjugate and $\Re$ real part).

The computation of these quantities in a bianisotropic layer is made by following in certain way the method developed in [22]. We start from Maxwell equations that can be written in each layer as:

$$\begin{bmatrix}[\mathcal{S}] & [0]\\ [0] & [\mathcal{S}]\end{bmatrix}_{(6\times6)}\cdot\begin{bmatrix}\boldsymbol{E}_i\\ \boldsymbol{H}_i\end{bmatrix} = j\omega\begin{bmatrix}-[\rho']_i & -[\mu]_i\\ [\epsilon]_i & [\rho]_i\end{bmatrix}_{(6\times6)}\cdot\begin{bmatrix}\boldsymbol{E}_i\\ \boldsymbol{H}_i\end{bmatrix} \tag{7}$$

with $[\mathcal{S}]$ being

$$[\mathcal{S}]_{(3\times3)} = \begin{bmatrix}0 & jk_z & \frac{\partial}{\partial y}\\ -jk_z & 0 & -jk_x\\ -\frac{\partial}{\partial y} & jk_x & 0\end{bmatrix}. \tag{8}$$

The second- and fifth-row equations in(7) are algebraic equations, and they can be used to eliminate E_y and H_y in terms of the remaining field components. Once the expressions of E_y and H_y have been found as linear functions of the other components, they can be introduced in (5) and (6) to rewrite the integrands as bilinear functions of $\boldsymbol{X}_i; \boldsymbol{X}_i^T = [E_x, E_z, H_x, H_z]_i$ (superscript T stands for transpose), that is

$$\big(E_xH_y^* - E_yH_x^*\big)_i = \boldsymbol{X}_i^{\mathrm{T}}\cdot[\boldsymbol{N}^z]_i\cdot\boldsymbol{X}_i^* \tag{9}$$

$$\big(E_yH_z^* - E_zH_y^*\big)_i = \boldsymbol{X}_i^{\mathrm{T}}\cdot[\boldsymbol{N}^x]_i\cdot\boldsymbol{X}_i^* \tag{10}$$

where $[\boldsymbol{N}^z]_i$ and $[\boldsymbol{N}^x]_i$ are (4×4) matrices that are explicitly written in Appendix B. Following the general treatment in [11], solutions for $\boldsymbol{X}_i(y)$ are given by

$$\boldsymbol{X}_i(y) = \exp(j\omega[\boldsymbol{Q}]_i y)\cdot\boldsymbol{X}_i(h_{i-1}) \qquad h_{i-1}\le y\le h_i \tag{11}$$

($[\boldsymbol{Q}]_i$ is a (4×4) matrix defined in [11]). Once k_z and k_x have been determined, $\boldsymbol{X}_i(y=0)$ is readily obtained from (2) with $\boldsymbol{E}_{t,0}^u = 0$ and the different $\boldsymbol{X}_i(y)$ computed using (11). Substituting now (9), (10), and (11) in (5) and (6), the transmitted power $\mathcal{P}_{z,x}^{(i)}$ is given by

$$\mathcal{P}_{z,x}^{(i)} = \frac{1}{2}\,\Re\int_{h_{i-1}}^{h_i}\Big(\boldsymbol{X}_i^{\mathrm{T}}(h_{i-1})\cdot\exp\Big(j\omega[\boldsymbol{Q}]_i^{\mathrm{T}}y\Big)\cdot[\boldsymbol{N}^{z,x}]_i \cdot\exp\big(-j\omega[\boldsymbol{Q}]_i^*y\big)\cdot\boldsymbol{X}_i^*(h_{i-1})\Big)\,dy. \tag{12}$$

We first diagonalize $[\boldsymbol{Q}]_i$ in order to compute (12), that is:

$$[\boldsymbol{Q}]_i = [\boldsymbol{D}]_i\cdot[\Lambda]^i\cdot[\boldsymbol{D}]_i^{-1} \tag{13}$$

with $[\boldsymbol{D}]_i$ being the diagonalization matrix of $[\boldsymbol{Q}]_i$ and $[\Lambda]$ a diagonal matrix whose elements are $\Lambda_{k,l}^i = \lambda_k^i\delta_{k,l}\big(\lambda_k^i,\ k=1,\cdots,4$ stand for the eigenvalues of matrix $[\boldsymbol{Q}]_i)$. If (13) is now substituted in (12), $\mathcal{P}_{z,x}^{(i)}$ can be rewritten, after some manipulations, as

$$\mathcal{P}_{z,x}^{(i)} = \frac{1}{2}\,\Re\Bigg\{\frac{j}{\omega}\sum_{k,l}\frac{a_{k,l}^i}{\lambda_k^i - \big(\lambda_l^i\big)^*}\cdot\Big[1-\exp\Big\{j\omega\Big(\lambda_k^i - \big(\lambda_l^i\big)^*\Big)\Big\}h_i\Big]\Bigg\} \tag{14}$$

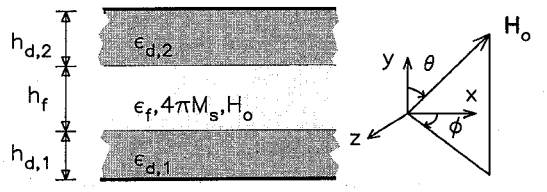

Fig. 2. Cross-section of a three ferrite-dielectric layer parallel-plate waveguide.

where

$$a^i_{k,l} = Y^i_k M^i_{kl} \left(Y^i_l\right)^* . \tag{15}$$

Y^i_k is the kth component of the four component vector

$$\boldsymbol{Y}^i = [\boldsymbol{D}]^{-1}_i \cdot \boldsymbol{X}_i(h_{i-1}) , \tag{16}$$

and $M^i_{k,l}$ the k,l elements of the (4×4) matrix

$$[\boldsymbol{M}]_i = [\boldsymbol{D}]^{\mathrm{T}}_i \cdot [\boldsymbol{N}^{z,x}]_i \cdot [\boldsymbol{D}]^*_i . \tag{17}$$

In numerical computations, the power flux has been normalized assuming the z-component of surface current density to be 1 mA/mm.

III. Numerical Results

The method of analysis developed in the previous sections is applied in this section to the study of the propagation of uniform modes in ferrite-loaded parallel plate waveguides magnetized at an arbitrary direction. As was pointed out in Section II-A, the present method is not restricted to this limitation. The specific structure to be analyzed is a three-layer parallel plate waveguide filled with a composite ferrite-dielectric medium (see Fig. 2). The losses and the exchange interaction effects are assumed to be negligible in the ferrite layer. The dielectric layer is also assumed lossless. These assumptions are made to emphasize the effects of the external magnetization field and to separate these effects from other possible ones (intrinsic anisotropy, exchange interactions, magnetic, or dielectric losses, etc.). Nevertheless, all these effects can be incorporated in the explicit expression of the magnetic permeability tensor by using the different models developed in the literature. The direction of the *internal* dc magnetization, $\boldsymbol{H}_0$, of the ferrite layer is defined by the spherical θ and ϕ angles. The $[\mu]$ tensor of the ferrite layer is assumed to be the Polder tensor [1] for this direction of the dc biasing field. Notice that the internal dc magnetic field does not correspond in general to the external dc magnetizing field, except a few particular configurations (see [1] and references therein).

As was mentioned above, the numerical computations have been restricted to the analysis of the so defined uniform modes (i.e., waves having a wave vector given by $\boldsymbol{k} = k_z \boldsymbol{a}_z + k_x \boldsymbol{a}_x = k_\xi \boldsymbol{a}_\xi$). This fact limits the possible complex values of k_z and k_x to those satisfying some of the following conditions ($\mathfrak{F}$ indicates imaginary part): 1) $\mathfrak{F}k_x/\mathfrak{F}k_z = \mathfrak{R}k_x/\mathfrak{R}k_z$, 2) $\mathfrak{R}k_x = 0, \mathfrak{R}k_z = 0$ or $\mathfrak{F}k_x = 0, \mathfrak{F}k_z = 0$, and 3) $k_x = 0, k_z \neq 0$ or $k_z = 0, k_x \neq 0$. The propagation constants of these modes for an arbitrary dc magnetization are computed by following the procedure outlined at the end of Section III-B. This procedure makes it possible to reduce the analysis of the aforementioned cases to the analysis of waves propagating along the $+z$-direction ($k_x = 0$) with different orientations of the internal dc biasing field. In this case $k_z = \beta - j\alpha$, with β being the phase constant and α the attenuation constant. The main reasons to restrict our numerical investigations to uniform modes are simplicity and the relevant information provided by this type of modes. A good insight in the microstrip or microslot transmission lines properties can be obtained from the analysis of the uniform modes propagating along the different parallel plate waveguides in which the transmission line can be subdivided. For example, the allowed k-band for the lateral nonradiating regime of a transmission line (at a given frequency) can be determined from this analysis. Notice also that in more general cases, it does not seem to be easy to plot the four quantities that determine the complex wave vector ($\boldsymbol{k} = k_z \boldsymbol{a}_z + k_x \boldsymbol{a}_x$) so that its physical interpretation becomes apparent. Finally, the theoretical interest itself of the uniform modes propagation characteristics justifies, in our opinion, its specific analysis.

Before analyzing particular structures, we have exhaustively checked our numerical results with those available in the literature. As an example, we have compared our results with those provided in [23], Fig. 2. Our numerical data have been computed assuming a very distant shielding conducting plate over the structure analyzed in [23]. The internal dc magnetizing field is fixed at two different orientations ($\theta = 90°, \phi = 45°$ and $\theta = 90°, \phi = 0°$). The frequency dependence of the propagation constants of the fundamental mode is depicted in Fig. 3 regarding $(+z)$ and $(-z)$ wave propagation. Some of electromagnetic data presented in [23, Fig. 2] when $\phi = \pm 45°, \pm 90°$ ($\phi = 45°, 0°$ in our notation) are reproduced in Fig. 3 (marked by the circles) as well as the magnetostatic limit results (dotted lines). The magnetostatic data have been obtained following the theory reported in [24] for the $\phi = 0°$ case. Note the good agreement between our data and the electromagnetic data of [23] at frequencies below about 4.2 GHz in the $\phi = 0°$ case. Our results for frequencies above 4.2 GHz clearly show how the mode depicted in [23, Fig. 2] is in fact the superposition of two modes (a forward electromagnetic wave (FEW) and a backward magnetostatic wave (BMW)) which gives rise to a nonreciprocal complex mode above 4.2 GHz. Power computations have been accomplished to support these considerations. Specifically, for complex modes, it has been verified that power flux in dielectric layers occurs in the direction of phase propagation. In ferrite layers, the power flux is opposite to the direction of phase propagation but it is equal in magnitude to that flowing through the dielectrics. An upper reciprocal TM mode (with the magnetic field polarized parallel to the internal dc bias field) appears at the analyzed frequency range, although it is not shown in the figure. The same considerations also can be applied to the $\phi = 45°$ case. Concerning the comparison between our electromagnetic data and the magnetostatic ones, it can be observed in Fig. 3 that both sets of data show the same qualitative behavior, even for the complex mode. In case the magnetostatic approximation can be assumed sufficiently valid, the numerical agreement

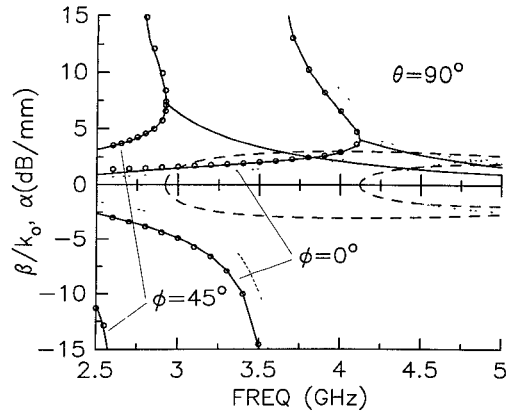

Fig. 3. Normalized phase constant β/k_0 :(_____) and attenuation factor α:(- - - - -) in dB/mm, magnetostatic limit: (·····), in a parallel-plate waveguide with $h_{d,1} = 1.27$ mm, $h_f = 2.03$ mm, $h_{d,2} \to \infty$, $\epsilon_{d,1} = 10.2$, $\epsilon_f = 17.5$, $\epsilon_{d,2} = 1$, $4\pi M_s = 2267$ G, $H_0 = 144$ Oe (o o oo) ([23, Fig. 2 data]).

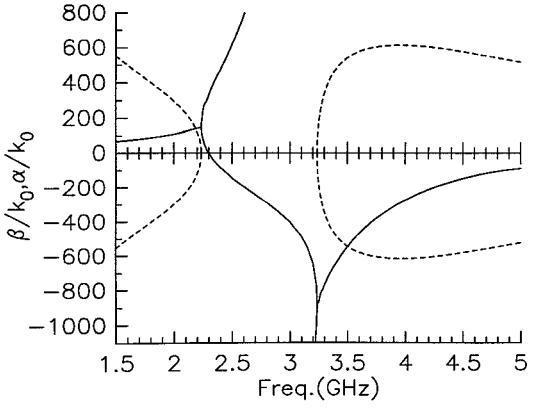

Fig. 4. Normalized phase constant β/k_0 :(_____) and normalized attenuation factor α/k_0:(- - - - -) in an air-ferrite-air parallel-plate waveguide with $h_{d,1} = 100\mu$ m, $h_f = 10\mu$ m, $h_{d,2} = 10\mu$ m, $\epsilon_f = 12.5$, $4\pi M_s = 1750$ G, $H_0 = 200$ Oe, $\phi = 0°$, $\theta = 90°$.

between our full-wave results and the magnetostatic one improves. This fact can be noted in Fig. 4, where a three thin layers dielectric-ferrite-dielectric structure is analyzed. Our results and those obtained using the magnetostatic formulas of [25] coincide, being indistinguishable in the graphic. This numerical coincidence is not surprising since the normalized phase constant $(\beta/k_0, k_0 = \omega/c)$ values of Fig. 4 are much higher than the ones of Fig. 3 (it is a well known fact that this condition leads to the magnetostatic approach [1]). This increase of the normalized phase constant values when the ferrite layer height decrease is reported in [26]. The magnetostatic complex values for the propagation constant plotted in Fig. 3 and in Fig. 4 have been obtained using the analytical extension to the complex plane of the implicit dispersion relations in [24] and [25]. It should be noticed that the magnetostatic approach can only predict certain part of the complete electromagnetic spectrum of the guides, namely the magnetostatic modes.

Fig. 5 shows the variations of the normalized phase constant, β/k_0, and the attenuation factor, α (dB/mm), of the fundamental mode of a two-layer dielectric-ferrite waveguide (assuming $h_{d,1} = 0$ in the structure shown in Fig. 2), when

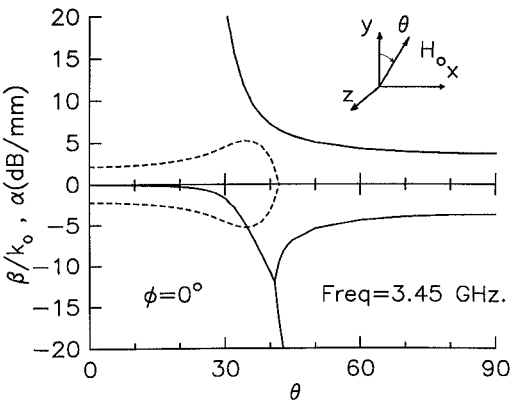

Fig. 5. Normalized phase constant β/k_0 :(_____) and attenuation factor α :(- - - - -) in dB/mm in a parallel-plate waveguide with $h_{d,1} = 0$, $h_f = 0.4$ mm, $h_{d,2} = 0.25$ mm, $\epsilon_f = 14.5$, $\epsilon_{d,2} = 12.5$, $4\pi M_s = 1600$ $4\pi M_s = 1600$ G, $H_0 = 500$ Oe, $\phi = 0°$.

the direction of the internal dc magnetization field is varied in the $x - y$ plane (namely $\theta = 0°$). The operating frequency is 3.45 GHz, and it lies within the forbidden frequency range for wave propagation in an infinite ferrite medium [1]. Note that wave propagation is reciprocal when $\theta = 0$ and $\theta = 90°$. In the $\theta = 0°$ case, the reciprocity is due to the symmetry of the structure. In the $\theta = 90°$ case, the wave propagation is reciprocal because the fundamental *electromagnetic* TM mode presents a polarization such that the magnetic field is aligned with the external biasing field. For other values of θ, the waveguide shows a strong nonreciprocal behavior. Complex and backward waves appear in this case when propagation is along $(-z)$ direction. The phase constant of the complex mode goes smoothly to zero when θ approach 0°, giving rise to two evanescent reciprocal waves. For propagation in the opposite direction, the fundamental TM_o mode becomes a forward magnetostatic wave (FMW) when θ decreases from 90°. Notice that purely evanescent modes $(\Re k = 0)$ do not occur except in the $\theta = 0°$ case (in which two reciprocal evanescent modes are present). This fact agrees with the general theorem shown in [21], which establishes that purely evanescent nonreciprocal modes are forbidden in transversely magnetized nonreciprocal waveguides (i.e., magnetized at any direction of the $(x - y)$ plane of the figure). In consequence, all nonreciprocal modes that do not carry a net average power flux in the direction of phase velocity must be complex.

Fig. 6 shows the effects of the variation of the direction of the internal dc bias field in the plane of the structure $(x - z$ plane, or $\theta = 90°)$. Qualitative results are very similar to the ones shown in Fig. 5, that is, complex and backward waves appear at certain intermediate values of the azimuthal angle. It is worth noting that purely evanescent modes occur only in case the wave propagation is reciprocal $(\theta = 90°)$. The nonappearance of evanescent nonreciprocal modes has been observed in all the analyzed nonreciprocal parallel plate waveguides regardless of the direction of magnetization. This fact suggest that the aforementioned theorem about transversely magnetized nonreciprocal waveguides [21], could be extended to nonreciprocal waveguides magnetized at an arbitrary direction. Nevertheless, we have not found a

TABLE I
NUMERICAL RESULTS CONCERNING POWER AND PROPAGATION CONSTANT OF THE BACKWARD AND COMPLEX MODES DEPICTED IN FIG. 7

Freq (GHz)	$\mathcal{P}_{z,d}(\mu w/\text{mm})$	$\mathcal{P}_{z,f}(\mu w/\text{mm})$	$\Re(P_y)(\mu w/\text{mm}^2)$	$\mathcal{P}_{x,d}(\mu w/\text{mm})$	$\mathcal{P}_{x,f}(\mu w/\text{mm})$	$k_z(\text{mm}^{-1})$
3.	$-0.5472 \cdot 10^4$	$0.1333 \cdot 10^5$	0	0	0	$(-2.676, 0)$
3.15	$-.9187 \cdot 10^2$	$0.1397 \cdot 10^3$	0	0	0	$(-1.071, 0)$
3.16	$-.7239 \cdot 10^2$	$0.7239 \cdot 10^2$	$\mp 0.2598 \cdot 10^2$	$\pm .2223 \cdot 10^3$	$\pm 0.2178 \cdot 10^3$	$(-0.9582, \pm 0.1794)$
3.5	$-0.1333 \cdot 10^2$	$0.1333 \cdot 10^2$	$\mp 0.1559 \cdot 10^2$	$\pm .2142 \cdot 10^3$	$\pm .2570 \cdot 10^3$	$(-0.2461, \pm 0.5849)$
4.	-1.324	1.324	∓ 0.7167	$\pm .2516 \cdot 10^2$	$\pm 0.3380 \cdot 10^2$	$(-0.0293, \pm 0.2706)$
4.4	-0.5240	0.5240	$\mp 0.3769 \cdot 10^{-1}$	± 1.903	± 2.587	$(-0.0128, \pm 0.0360)$
4.41	-0.3560	0.7319	0	0	0	$(-0.8720 \cdot 10^{-2}, 0)$
4.42	0.9683	2.522	0	0	0	$(0.2378 \cdot 10^{-1}, 0)$
4.5	3.793	6.230	0	0	0	$(0.9484 \cdot 10^{-1}, 0)$

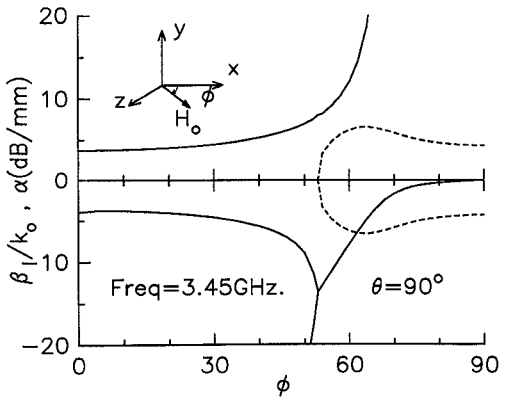

Fig. 6. Normalized phase constant β/k_0 :(_____) and attenuation factor α :(- - - - -) in dB/mm in a parallel-plate waveguide with $h_{d,1} = 0$, $h_f = 0.4$ mm, $h_{d,2} = 0.25$ mm, $\epsilon_f = 14.5$, $\epsilon_{d,2} = 12.5$, $4\pi M_s = 1600$ G, $H_0 = 500$ Oe, $\theta = 90°$.

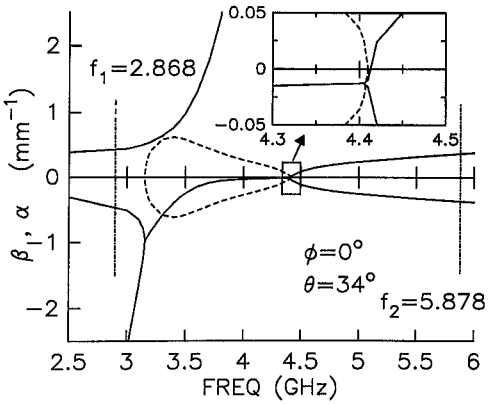

Fig. 7. Phase constant $\beta(\text{mm}^{-1})$:(_____) and attenuation constant $\alpha(\text{mm}^{-1})$ ::(- - - - -) in a parallel-plate waveguide with $h_{d,1} = 0$, $h_f = 0.4$ mm, $h_{d,2} = 0.25$ mm, $\epsilon_f = 14.5$, $\epsilon_{d,2} = 12.5$, $4\pi M_s = 1600$ G, $H_0 = 500$ Oe, $\phi = 0°, \theta = 34°$.

general proof of such general theorem for an arbitrary dc magnetization yet.

The dispersion characteristics of the fundamental mode of the waveguide of Fig. 5 are plotted in Fig. 7. The internal angles of the dc magnetization are $\theta = 34°$ and $\phi = 0°$ so that the complex nature of the analyzed mode can be easily appreciated. Strong nonreciprocity as well as complex and backward modes appear at frequencies within the forbidden frequency range for plane wave propagation in a transversely magnetized infinite ferrite medium ($\omega_1 < \omega < \omega_2; \omega_1 = \sqrt{\{\omega_0(\omega_0 + \omega_m)\}}, \omega_2 = \omega_0 + \omega_m$) [1]. It is observed from the figure that the mode appearing at 2.5 GHz, with positive phase constant, is turning into an FMW when frequency increases. The propagating mode with negative phase constant at 2.5 GHz encounters a BMW at 3.155 GHz and they join together to produce a nonreciprocal complex wave NCW. This complex wave disappears above 4.405 GHz giving rise now to a FEW and a backward electromagnetic wave BEW that quickly becomes a FEW. This transition to a forward wave occurs after the propagation constant passes through zero at 4.414 GHz. Above this frequency, two slightly nonreciprocal FEW propagate.

Power computations for the backward and complex modes depicted in Fig. 7 are shown in Table I. Special attention has been paid to the frequency range in which the transition from backward to NCW occurs. The real part of the y-component of the Poynting vector $\Re(P_y)$ at the dielectric-ferrite interface is also shown. It can be checked that power flows from the dielectric to the ferrite layers in the exact amount to compensate the attenuation, that is: $\Re(P_y) = (\partial/\partial z)\text{P}_z = 2\alpha\mathcal{P}_z$. Both the backward and complex waves carry a power flux $\mathcal{P}_z$ through the dielectric layer in a direction parallel to the phase velocity, and in the opposite direction inside the ferrite layer (see Table I). Actually, this result has been checked in all the computed structures, that is, $\mathcal{P}_z$ flows through dielectric layers in the same direction as the wavefronts and through ferrite layers in opposite direction (for backward and complex modes). A nonzero transmitted power in the transverse direction $\mathcal{P}_x$ is present in Table I for the complex modes. Notice that this direction is the only allowed one for power transmission owing to the nature of the complex mode.

Complex modes in reciprocal waveguides have been widely analyzed [14]–[17], [19]. These modes have been grouped together into two pairs with propagation constants $\pm\beta - j\alpha$ and $\pm\beta + j\alpha$, respectively. Each one of these pairs would be excited in a discontinuity (with the appropriate sign of α), with the members of the exited pair strongly coupled in the energy sense [16]. The presence of complex modes propagating only in one direction, with propagation constant $\beta \pm j\alpha$ or (rather than *and*) $-\beta \pm j\alpha$, is a direct consequence of the *nonreciprocity* of the wave propagation. Therefore, the pairs of complex modes suggested in [16] have not any sense here because there are not two different and opposite values for the real part of the propagation constant among the complex

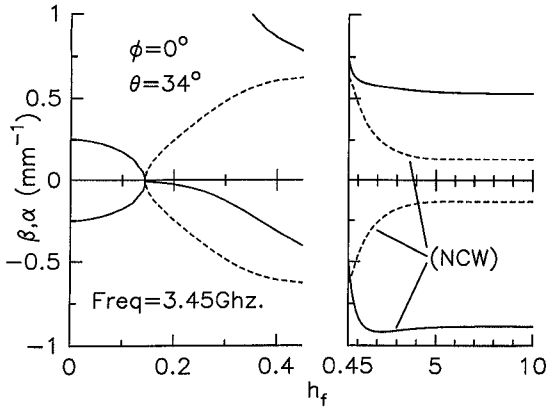

Fig. 8. Phase constant $\beta(\mathrm{mm}^{-1})$:(_____) and attenuation constant $\alpha(\mathrm{mm}^{-1})$ ::(- - - - -) versus the ferrite height in a parallel-plate waveguide with $h_{d,1} = 0$, $h_{d,2} = 0.25$ mm, $\epsilon_f = 14.5$, $\epsilon_{d,2} = 12.5$, $4\pi M_s = 1600$ G, $H_0 = 500$ Oe, $\phi = 0°, \theta = 34°$.

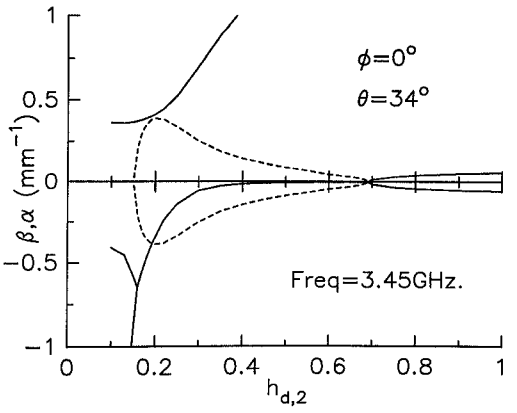

Fig. 9. Phase constant $\beta(\mathrm{mm}^{-1})$:(_____) and attenuation constant $\alpha(\mathrm{mm}^{-1})$ ::(- - - - -) versus the dielectric height in a parallel-plate waveguide with $h_{d,1} = 0, h_f = 0.4$ mm, $\epsilon_f = 14.5$, $\epsilon_{d,2} = 1$, $4\pi M_s = 1600$ G, $H_0 = 500$ Oe, $\phi = 0°, \theta = 34°$.

solutions. Assuming that nonreciprocal complex modes are excited in a discontinuity of a nonreciprocal waveguide, it is expected that *each* member of the *single* pair of NCW present in the waveguide could be excited separately (with the appropriate sign of the attenuation constant α). Nevertheless, despite of the presence of a single complex wave of the pair at the discontinuity, there is not any contradiction concerning the energy associated to this wave since power flux computations have made it evident that the same amount of power flows in opposite directions through the ferrite and the dielectric layers in NCW. A similar result was previously reported in [15] for reciprocal complex modes propagating in rectangular dielectric image guides.

Fig. 8 shows the effect of the height of the ferrite layer on the propagation characteristics of the analysed complex mode. Thus, it can be observed that the propagation constant of the complex wave remains almost unchanged when the height of the ferrite layer increases above 5 mm, approximately. This fact suggests that the complex waves are mainly associated to the ferrite-dielectric interface. This very interpretation is also provided by the analysis of the transmitted power through the ferrite layer. This quantity remains practically unchanged when the ferrite layer thickness increases above 5 mm. Nevertheless, the effect of the ferrite layer thickness is significant for thin ferrite layers: the complex wave disappear below about 0.145 mm. Another mode also appears in the figure when the ferrite-layer height is above 0.3 mm approximately. This mode starts being a FMW to turn into a FEW when height increases.

The effects of the dielectric permittivity of the dielectric layer have also been analyzed although they will not be shown. It has been found that the qualitative behavior of the fields is not significantly affected by this parameter. Fig. 9 shows the effect of the dielectric layer height on the propagation constants of the two nonreciprocal fundamental modes appearing at 3.45 GHz with $\theta = 34°$. Note that the upper ground plane distance strongly affects the behavior of the fields when the dielectric height is below about 0.8 mm. In turn, this distance hardly affects for heights above 0.8 mm.

Fig. 10 displays the variations of the propagation constant of a symmetrical three-layers (dielectric-ferrite-dielectric) waveguide ($h_{d,1} = h_{d,2}$ in Fig. 2) at 3.45 GHz when the direction of the internal dc magnetization changes in the $x - z$ plane ($\theta = 90°$). The wave propagation is reciprocal, because the guide, including the dc magnetic biasing field, has inversion symmetry with respect to any point at the horizontal middle plane. Two pairs of reciprocal complex waves RCW appear now at certain intermediate values of the azimuthal angle. A comparison with the two-layers configuration shows that the real part of the complex propagation constant of the RCW does not go to zero smoothly when ϕ increases (see Fig. 6). In turn, the real part of k_z goes steeply to zero, each pair of reciprocal complex modes giving rise to two evanescent reciprocal waves. This latter result is in agreement with the aforementioned theorem [21] for reciprocal and nonreciprocal nonpropagating modes in gyromagnetic inhomogeneously filled waveguides, namely, reciprocal purely evanescent modes are allowed, but nonreciprocal purely evanescent ones are forbidden and must be complex for all frequencies.

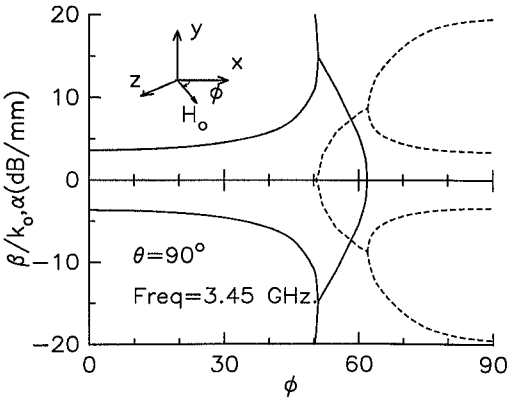

Fig. 10. Normalized phase constant β/k_0 :(_____) and attenuation factor α :(- - - - -) in dB/mm in a parallel-plate waveguide with $h_{d,1} = 0.25$ mm, $h_f = 0.4$ mm, $h_{d,2} = 0.25$ mm, $\epsilon_{d,1} = 12.5$, $\epsilon_{d,2}$, $\epsilon_f = 14.5$, $4\pi M_s = 1600$ G, $H_0 = 500$ Oe, $\theta = 90°$.

IV. Conclusions

We have presented a systematic method to obtain the propagation characteristics of *electromagnetic* waves propagating in

bianisotropic multilayered parallel plate waveguides. Special care has been paid to the obtaining of the dispersion relation of the waveguide in terms of the complex roots of an *analytical* function. An efficient integral method is then employed to find these complex zeros. This method makes it possible to overcome all the drawbacks regarding the handling of meromorphic functions. Following the aforementioned searching procedure, *all* the complex propagation constants lying within a given region of the complex plane can be readily obtained. A systematic procedure to compute the power flow has also been developed.

The method developed here to solve the characteristic equation and to obtain the transmitted power has been used to investigate the modal spectrum of lossless parallel-plate waveguides loaded with ferrite layer arbitrarily magnetized. This investigation has been restricted to the analysis of *uniform modes,* i.e., modes that propagate along a given direction in the plane of the waveguide, being uniform in the direction orthogonal to propagation. The numerical results have been checked both with previous one reported in the literature and with those obtained by solving the magnetostatic approach formulas (assumed to be valid). A good agreement has been found in all cases. Nevertheless, the comparison with previous results has been restricted to propagating modes only since no previous information about complex modes in this type of waveguides has been found.

The numerical investigation has revealed that the transition between forward and backward waves always leads to the appearance of a complex wave. In case the magnetostatic approach is assumed to be valid, the complex propagation constant of magnetostatic complex modes can be calculated by using the analytical extension to the complex plane of the magnetostatic implicit dispersion relation for propagating waves. When the forward and backward modes are nonreciprocal, the resulting complex modes are equally nonreciprocal, appearing as a pair of waves with an $\exp(-jk_z z)$-dependence with *complex* conjugate propagation constants k_z and k_z^*.

In two-layers ferrite-dielectric parallel plate waveguides, it has been found that he fundamental electromagnetic mode becomes complex when the waveguide is subjected to an oblique dc magnetization. Such a transformation of the propagating fundamental mode into a complex mode has been observed at frequencies included within the *forbidden* frequency range for wave propagation in an infinite lossless ferrite medium. It has also been found that a complex mode in such two-layer structures appears and disappears turning into forward and backward propagating waves. Nonreciprocal purely evanescent modes are not present in the investigated waveguides. All the nonreciprocal modes that do not carry a net average power flux in the direction of the phase propagation are complex modes. This latter result is in agreement with previous results reported by the authors [21].

Power computations have shown that power flux through the dielectric layers is always in the same direction as the phase propagation. On the contrary, the power flux of complex and backward waves through ferrite layers occurs in the opposite direction to the phase propagation. The total power transmitted by complex modes is found to be null in the direction of the phase propagation.

The aforementioned transformation of the fundamental modes in complex waves has also been found in reciprocal dielectric-ferrite-dielectric waveguides magnetized at an oblique direction. These modes show complex reciprocal propagation constants of the type $k_z = \pm\beta \pm j\alpha$. Since the wave propagation is reciprocal, reciprocal evanescent modes are also present together with the reciprocal complex modes.

APPENDIX A

It is a well known fact from the diffraction theory that if $\psi(\boldsymbol{r})$ is a function that satisfies the Helmholtz equation inside a closed surface S and if ψ and $(\partial/\partial_n)\psi$ are zero over a finite part of S, then ψ is zero at all points of the space enclosed by S [27]. This theorem shows that if $\boldsymbol{n} \times \boldsymbol{E}$ and $\boldsymbol{n} \times \boldsymbol{H}$ are zero on a finite part of a closed surface enclosing a homogeneous, *isotropic,* and source-free region, all the fields are zero at all points inside this region. To extend this theorem to homogeneous but *anisotropic* media, we can proceed as follows:

Theorem: Let a source-free bianisotropic homogeneous medium bounded by a closed surface S. If $\boldsymbol{n} \times \boldsymbol{E}$ and $\boldsymbol{n} \times \boldsymbol{H}$ are assumed to be zero on a finite surface $S_1 \subset S$, then $\boldsymbol{E}$ and $\boldsymbol{H}$ are zero at any points enclosed by S.

Proof: Let $P_1(x, y, z)$ be a point on S_1 (see Fig. 11). From the Maxwell equations it is followed for the normal component of the $\boldsymbol{B}(P_1)$ fields that

$$-j\omega B_n(P_1) = \frac{\partial E_v}{\partial u} - \frac{\partial E_u}{\partial v} = 0$$
$$j\omega D_n(P_1) = \frac{\partial H_v}{\partial u} - \frac{\partial H_u}{\partial v} = 0\,. \tag{18}$$

If the constitutive relation written in the coordinate system (u, v, n), i.e.,

$$\begin{bmatrix} \boldsymbol{D} \\ \boldsymbol{B} \end{bmatrix} = [\boldsymbol{M}] \cdot \begin{bmatrix} \boldsymbol{E} \\ \boldsymbol{H} \end{bmatrix} \tag{19}$$

is combined with the starting hypothesis taking into account (18), the second and fifth equaitons in (19) are rewritten as:

$$0 = m'_{22}E_n + m'_{25}H_n$$
$$0 = m'_{52}E_n + m'_{55}H_n \tag{20}$$

giving rise to

$$E_n = H_n = 0 \tag{21}$$

assuming the determinant in (20) is not zero. Thus, incorporating (21) in (19) and taking into account that $\boldsymbol{n} \times \boldsymbol{E} = 0$ and $\boldsymbol{n} \times \boldsymbol{H} = 0$ on S_1, it follows that

$$\boldsymbol{E}(P_1) = \boldsymbol{D}(P_1) = \boldsymbol{H}(P_1) = \boldsymbol{B}(P_1) = 0\,. \tag{22}$$

Since surface S_1 is *finite,* all the field tangential derivatives of any order are also cancelled, that is

$$\frac{\partial^q A_i(P_1)}{\partial u^q} = \frac{\partial^q A_i(P_1)}{\partial v^q} = 0 \tag{23}$$

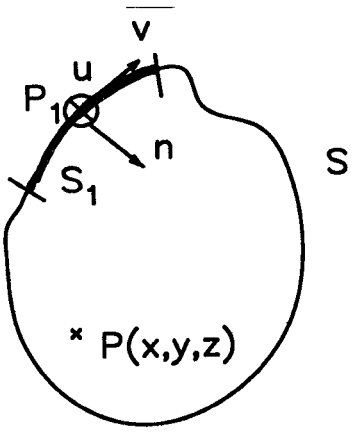

Fig. 11. A closed surface enclosing a bianisotropic and homogeneous medium.

where $A_i(P_1)(1 \leq i \leq 6)$ stands for one of the six component of the $[\boldsymbol{D}, \boldsymbol{B}]$ or $[\boldsymbol{E}, \boldsymbol{H}]$ field.

Owing to the Maxwell equations are linear equations of first order, the normal derivative of any field is given by:

$$\frac{\partial A_i(P_1)}{\partial n} = \sum_{j=1}^{6} \left(\mathcal{P}_{ij} A_j + Q_{ij} \frac{\partial A_j}{\partial u} + R_{ij} \frac{\partial A_j}{\partial v} \right) \quad (24)$$

with $\mathcal{P}_{ij}, Q_{ij}$, and R_{ij} being constants that depend on the characteristics of the medium. It is obvious from (24) that any normal field derivative or order q can be expressed in terms of the fields and its tangential derivative of orders $1, 2, \cdots, q$. Hence, all the normal field derviatives together with any crossfield derivative are null provided S_1 is finite

$$\frac{\partial^q A_i(P_1)}{\partial n^q} = 0. \quad (25)$$

Let $P(x, y, z)$ be an arbitrary point inner to S. From the application of the Taylor theorem, the electromagnetic field in $P, A_i(P)$ can be determined in terms of $A_i(P_1)$ and its derivatives. Since the electromagnetic field and all its derivatives are null in P_1, the field in P is null.

Let us now consider that the medium bounded by S is piece-wise homogeneous. The above theorem shows that the electromagnetic field is null inside the homogeneous region in contact with S_1. If the tangential continuity of $\boldsymbol{E}$ and H over the surface bounding this homogeneous region is taking into account, the successive application of the above theorem leads to a null field in all the region enclosed by S.

APPENDIX B

In case the layer considered does not have optic activity ($[\rho']_i = 0, [\rho]_i = 0$) and $k_x = 0$, $[\boldsymbol{N}^z]$ and $[\boldsymbol{N}^x]$ matrices are given by

$$[\boldsymbol{N}^z] = \begin{bmatrix} \frac{k_z^*}{\omega \mu_{22}^*} & 0 & \left(\frac{\epsilon_{21}}{\epsilon_{22}} - \frac{\mu_{21}^*}{\mu_{22}^*} \right) & -\frac{\mu_{23}^*}{\mu_{22}^*} \\ 0 & 0 & \frac{\epsilon_{23}}{\epsilon_{22}} & 0 \\ 0 & 0 & \frac{k_z^*}{\omega \epsilon_{22}} & 0 \\ 0 & 0 & 0 & 0 \end{bmatrix} \quad (26)$$

$$[\boldsymbol{N}^z] = \begin{bmatrix} 0 & 0 & 0 & -\frac{\epsilon_{21}}{\epsilon_{22}} \\ -\frac{k_z^*}{\omega \mu_{22}^*} & 0 & \frac{\mu_{21}^*}{\mu_{22}^*} & \left(\frac{\mu_{21}^*}{\mu_{22}^*} - \frac{\epsilon_{23}}{\epsilon_{22}} \right) \\ 0 & 0 & 0 & \frac{k_z^*}{\omega \epsilon_{22}} \\ 0 & 0 & 0 & 0 \end{bmatrix} \quad (27)$$

where $\mu_{k,l}$ and $\epsilon_{k,l} k, l = 1, 2, 3$ stand for the orthogonal components of the constitutive tensors $[\mu_i]$ and $[\epsilon_i]$ in the considered coordinate system (x, y, z), and the superscript * stands for the complex conjugate.

REFERENCES

[1] M. S., Sodha, N. C. Srivastava, *Microwave Propagation in Ferrimagnetics.* New York: Plenum Press, 1981.

[2] H. Unz, "Propagation in arbitrarily magnetized ferrites between two conducting parallel planes," *IEEE Trans. Microwave Theory Tech.,* vol. MTT-12, pp. 204–210, May 1964

[3] F. Bardati and P. Lampariello, "The modal spectrum of a lossy ferrimagnetic slab," *IEEE Trans. Microwave Theory Tech.,* vol. MTT-27, pp. 679–688, July 1979.

[4] I. Awai, T. Itho, "Coupled-mode theory analysis of distributed nonreciprocal structures," *IEEE Trans. Microwave Theory Tech.,* vol. MTT-29, pp. 1077–1086, Oct. 1981.

[5] M. Mrozowski, and J. Mazur, "General analysis of parallel-plate waveguide inhomogeneously filled with gyromagnetic media," *IEEE Trans. Microwave Theory Tech.,* vol. MTT-34, pp. 388–395, Apr. 1986.

[6] N. C. Srivastava, "Surface wave propagation through a small gap between oppositely magnetized ferrite substrates," *IEEE Trans. Microwave Theory Tech.,* vol. MTT-26, pp. 213–215, Mar. 1978.

[7] S. C. Tsalamengas and N. K. Uzunoglu, "Radiation from a dipole in the proximity of a general anisotropic grounded layer," *IEEE Trans. Ant. Prop.,* vol. AP-33, pp. 165–172, Feb. 1985.

[8] F. Mesa, R. Marqués, and M. Horno, "An efficient numerical method to analyse a large class of nonreciprocal planar transmission lines," *IEEE Trans. Microwave Theory Tech.,* vol. MTT-40, pp. 1630–1640, Aug. 1992.

[9] N. K. Das and D. M. Pozar, "Full-wave spectral-domain computation of material, radiation, and guided wave losses in infinite multilayered printed transmission lines," *IEEE Trans. Microwave Theory Tech.,* vol. MTT-39, pp. 54–63, Jan. 1991.

[10] F. Mesa, R. Marqués, and M. Horno, "Complete modal spectrum of nonreciprocal multilayered microstrip lines," *URSI International Symposium on Electromagnetic Theory,* pp. 397–399, Sidney, Australia, Aug. 1992.

[11] ——, "A general algorithm for computing the bidimensional spectral dyadic Green's function: The equivalent boundary method (EBM)" *IEEE Trans. Microwave Theory Tech.,* pp. 1640–1649 Sept. 1991.

[12] L. M. Delves, and J. N. Lyness, "A numerical method for locating the zeros of an analytic function," *Math. Comput.,* vol. 21, pp. 543–560, 1967.

[13] F. L. Mesa, "Study of the electromagnetic propagation characteristics in multiconductor lines of planar configuration embedded in bianisotropic layered media," Ph.D. dissertation (in Spanish), Universidad de Sevilla, 1991.

[14] P. J. B. Clarricoats and K. R. Slinn, "Complex modes of propagation in dielectric-loaded circular waveguides," *Electronics Lett.,* vol. 1, no. 5, pp. 145–146, July 1965.

[15] U. Crombach, "Complex waves on shielded lossless rectangular dielectric image guide," *Electronics Lett.,* vol. 19, no. 14, pp. 557–558, July 1983.

[16] A. S. Omar and K. Schünemann, "Formulation of the singular integral equation technique for planar transmission lines," *IEEE Trans. Microwave Theory Tech.,* vol. MTT-33, pp. 1313–1321, Dec. 1985.

[17] W. Huang and T. Itho, "Complex modes in losses shielded microstrip lines," *IEEE Trans. Microwave Theory Tech.,* vol. MTT-36, pp. 163–165, Jan. 1988.

[18] R. Marqués and M. Horno, "An exact method for analyzing boxed microstrips on lossy substrates," *Microwave and Optical Tech. Letters,* vol. 2, no. 2, pp. 39–43, Feb. 1989.

[19] A. S. Omar and K. Schünemann, "Complex and backward-wave modes in inhomogeneously and anisotropically filled waveguides," *IEEE Trans. Microwave Theory Tech.,* vol. MT-35, pp. 268–275, Mar. 1987.

[20] C.-K. C. Tzuang, C.-Y. Lee, and J.-T. Kuo, "Complex modes in lossless nonreciprocal finlines," *Electronic Lett.,* vol. 26, no. 22, pp. 1919–1921, Oct. 1990.

[21] R. Marqués, F. Mesa, M. Horno, "On the complex nature of higher order modes in lossless nonreciprocal transversely magnetized waveguides," *IEEE Microwave Wave Guided Lett.,* vol. 2, no. 7, pp. 278–280, July 1992.
[22] G. Cano, F. Medina, and M. Horno, "Characteristic impedance of microstrip and finline on layered biaxial substrates," *Microwave Optical Lett.,* vol. 2, no. 6, pp. 210–214, 1989.
[23] E. El-Sharawy and R. W. Jackson, "Fullwave analysis of an infinitely long magnetic surface wave transducer," *IEEE Trans. Microwave Theory Tech.,* vol. MTT-38, pp. 730–737, June 1990.
[24] W. L. Bongianni, "Magnetostatic propagation in a dielectric layered structure," *J. Appl. Physic,* vol. 43, no. 6, pp. 2541–2548, Jan. 1972.
[25] T. Yukawa and J. Ikenoue, "Effects of metal on dispersion relations on magnetostatic volume waves," *J. Appl. Physic,* vol. 49, no. 1, pp. 376–382, Jan. 1978.
[26] R. Rupin, "Electromagnetic modes for a ferromagnetic slab," *J. Appl. Physic,* vol. 62, pp. 11–15, July 1987.
[27] J. A. Stratton, *Electromagnetic theory,* New York: McGraw-Hill 1941, p. 463.

Ricardo Marqués, photograph and biography not available at time of publication.

Francisco L. Mesa, photograph and biography not available at time of publication.

Manuel Horno, photograph and biography not available at time of publication.